6th European Conference on Computational Mechanics (ECCM 6)
7th European Conference on Computational Fluid Dynamics (ECFD 7)
11–15 June 2018, Glasgow, UK

# MATHEMATICAL MODELLING OF STRUCTURAL HEALTH MONITORING SYSTEMS: COUPLING FLUID-STRUCTURE INTERACTION WITH WAVE PROPAGATION.

**Bhuiyan Shameem Mahmood Ebna Hai**[1] **and Markus Bause**[2]

[1,2] Chair of Numerical Mathematics
Faculty of Mechanical Engineering
Helmut Schmidt University
University of the Federal Armed Forces Hamburg
Holstenhofweg 85, 22043 Hamburg, Germany.
{ebnahaib, bause}@hsu-hh.de

**Key words:** Multiphysics, fluid-structure interaction, Galerkin finite element method, wave propagation, structural health monitoring system.

**Abstract.** In this contribution, a novel concept of coupling Fluid-Structure Interaction (FSI) with an ultrasonic wave propagation is proposed. It is referred to as extended Fluid-Structure Interaction (eXFSI) problem. The eXFSI is a one-directional coupling of typical FSI problem with an ultrasonic wave propagation in fluid-solid and their interaction (WpFSI). The WpFSI is a strongly coupled problem of acoustic and elastic wave equations, where FSI problem solution feeds in automatically the boundary condtions at each time step. The principal aim of this research is the exploration and development of concepts for the efficient numerical solution of the eXFSI problem. The finite element method is used for the spatial discretization. Temporal discretization is based on finite differences and is formulated as a one step-$\theta$ scheme, from which we can consider shifted Crank-Nicolson and the fractional-step-$\theta$ schemes. The nonlinear problem is solved by a Newton-like method. To demonstrate the application of the eXFSI and WpFSI models, we elaborate on the design of the on-live and off-live Structural Health Monitoring (SHM) systems for composite material and lightweight structure, respectively. The implementation is accomplished via the software library package DOPELIB.

## 1 INTRODUCTION

Mathematical modeling for the purpose of engineering implementation requires both comprehensive mimicing of the physical system, but also computational efficiency. Here, we explore the caveats of mathematical modeling and numerical solution of the problem that is a part of Structural Health Monitoring (SHM) system. In other words, we focus on the computational side of the SRM system, which is indeed closely tied to the hardware part of SHM system. The ultimate benefit of using the SHM system is the ability of damage idenftification under the principle of non-destructive testing. The applications include, but are not limited to, mechanical, aerospace, or civil engineering infrastructures. In the present work, we contribute to the rather

sparse literature on computational techniques, which support the SHM process. In particular, we explore modeling caveats of the so-called on-line SHM system. The on-line SHM system tracks the structural integrity throughout the operation of the object under consideration. The model developed in the present work can be employed in a varies structures e.g. bridge, airplane during the flight, wind turbine. The differences would come in the parametrization. To this end, most studies that analyze SHM system are experimental. Thereby, proposing the novel model, we ensure the credibility of our results by contrasting them to the experimental data.

In a nutshell, the mathematical model we develop couples the wave propagation phenomena with the fluid-solid interaction (FSI) problem. It comprises wave-propagation-based methods and falls under the FSI problems category. Thereby, we rely upon fundamental pronciples of the FSI theory. Numerical solution of the FSI problem calls for resolving both fluid flow and elastic structural deformations. The associated complexity drives the need for the monolithic approach, which emerged over the past few years as a first-choice methodology for multi-physica problems. Overall, the FSI simulations have contributed to a better understanding e.g. of the convective flow, pressure fields, and deformation through the solution of the nonlinear multi-physics problems. Moreover, the fact that the FSI effect may jeopordize structural integrity justifies the efforts put into its comprehensive solution (cf. [1, 2, 3, 4, 17, 18]). In the framework of eXFSI, the following two models are coupled (cf. [5, 6, 7, 8, 9, 10, 11, 12, 14]):

- Nonlinear FSI in the ALE framework. This includes the incompressible Navier-Stokes in the ALE framework, non-linear elastodynamics in Lagrangian framework, and the biharmonic mesh moving model;
- Nonlinear wave propagation (WpFSI) problem in the ALE framework, which is a coupled problem of the time-harmonic elastic wave propagation with a signal force in the ALE framework, and acoustic wave propagation in the ALE framework.

In the nonlinear FSI model, we deal with three types of nonlinearities: fluid convection, a geometrically nonlinear Green-Lagrange strain tensor, and the nonlinear ALE mapping. With regard to the second model, we emphasise that we consider a strongly coupled time-harmonic acoustic and elastic wave problem in the ALE framework in order to account for the structural deformation due to the FSI effect. The eXFSI is solved via monolithic technique. To combine two alternative settings – Eulerian and the Lagrangian – we rely upon the ALE framework. A basic partitioned approach does not contain a variational equation for the eXFSI problem. Therefore, we introduce an auxiliary coordinate transformation function $\hat{\mathcal{T}}$ (i.e. the ALE mapping) for the Eulerian setting. The ALE approach provides a simple procedure to couple solid deformations with fluid flows by a monolithic solution algorithm. In such a setting, the fluid flow and wave propagation problems are transformed to a reference configuration by the ALE mapping. To sum up, the novelties of the present work are two-fold.

- First, we propose the FE-based on-live SHM model eXFSI. It merges a coupled wave propagation problem in the ALE framework and the FSI model. By means of eXFSI, we investigate the wave propagation in a dynamic structure. To mimic the latter, we introduce the fluid flow, which alters the elastic beam. Thereby, we are also dealing with

the dynamic boundary conditions. The dynamic boundary conditions, in turn, alter the wave propagation.

- Second, we propose a dual linear solving technique to address the eXFSI problem using monolithic algorithm.

## 2 NOTATION AND FUNCTION SPACE

Here, we introduce the domain, where the interactions between the two phases of a matter, i.e. fluid and solid, are explored. Let us consider the time interval $I = [0, T]$ with $T > 0$. The domain $\Omega(t) \subset \mathbb{R}^d$, with $d \in \{2, 3\}$, is open, connected, bounded, and varies with time $t \in I$. The domain comprises two time-dependent subdomains $\Omega_f(t)$ (fluid part) and $\Omega_s(t)$ (solid part): $\Omega(t) = \Omega_f(t) \cup \Omega_s(t)$. (cf. Figure 1). The two subdomains do not overlap i.e. $\Omega_f(t) \cap \Omega_s(t) = \emptyset$. Furthermore, the domain $\Omega(t)$ has a Lipschitz boundary $\partial\Omega(t) \subset \mathbb{R}^{d-1}$, which is subdivided into four parts as follows: $\partial\Omega(t) = \partial\Omega_{in}(t) \cup \partial\Omega_{wall}(t) \cup \partial\Omega_{base}(t) \cup \partial\Omega_{out}(t)$, where $\partial\Omega_{in}(t)$, $\partial\Omega_{wall}(t)$ and $\partial\Omega_{base}(t)$ are Dirichlet boundaries (for the velocities and displacements) and $\partial\Omega_{out}(t)$ denotes the fluid outflow Neumann boundary. The fluid-solid interface i.e. boundary between the solid and fluid $\partial\Omega_i(t) \subset \mathbb{R}^{d-1}$ is given by: $\partial\Omega_i(t) = \overline{\Omega_f}(t) \cap \overline{\Omega_s}(t)$. The outward normal vectors of fluid and solid at the fluid-solid interface are denoted by $n_f$ and $n_s$, respectively. The initial (henceforth reference) domains, i.e. at $t = 0$, are denoted by $\hat{\Omega}_f$ and $\hat{\Omega}_s$. Here, the fluid boundary $\partial\hat{\Omega}_f \subset \mathbb{R}^{d-1}$ and solid boundary $\partial\hat{\Omega}_s \subset \mathbb{R}^{d-1}$ are given by: $\partial\hat{\Omega}_f = \partial\hat{\Omega}_i \cup \partial\hat{\Omega}_{fD} \cup \partial\hat{\Omega}_{fN}$, and $\partial\hat{\Omega}_s = \partial\Omega_i \cup \partial\hat{\Omega}_{sD}$. Accordingly, the initial common interface boundary $\partial\hat{\Omega}_i \subset \mathbb{R}^{d-1}$ is referred to by $\partial\hat{\Omega}_i = \overline{\hat{\Omega}_f} \cap \overline{\hat{\Omega}_s}$, and the corresponding outward normal vectors at the fluid-solid interface are denoted by $\hat{n}_f$ and $\hat{n}_s$. The fluid, solid and wave displacements and velocities are set to zero on $\partial\hat{\Omega}_D$. On $\partial\hat{\Omega}_{out}$, the displacements are presumed to be zero. The prestressed configuration presumes the application of the stress prior to the reference time $t = 0$. This implies possible deformation already at time $t = 0$. The choice of the initialisation is application-dependent. Since we are using a variational monolithic coupling method [4, 5, 6, 8, 10, 11, 12, 17], the displacements and velocity spaces are extended to the entire domain $\hat{\Omega}$. For the eXtended Fluid-Structure Interaction (eXFSI) problem, we work with the following spaces:

$$\begin{aligned} \hat{L}_{\hat{\Omega}_X} &:= L^2(\hat{\Omega}_X), \qquad & \hat{L}^0_{\hat{\Omega}_X} &:= L^2(\hat{\Omega}_X)/\mathbb{R}, \\ \hat{V}_{\hat{\Omega}_X} &:= H^1(\hat{\Omega}_X), \qquad & \hat{V}^0_{\hat{\Omega}_X} &:= H^1_0(\hat{\Omega}_X). \end{aligned} \tag{1}$$

Here, $X = \{s, f\}$ is a set of suffixes: "$f$" stands for the fluid and "$s$" stands for the solid domain. For convenience, we omit the explicit time-dependence term when indicating the time-dependent domains i.e. $\Omega := \Omega(t)$. Last but not least, for the current domains $\Omega$, $\Omega_f$ and $\Omega_s$, we can denote the corresponding spaces without the hat ($\hat{}$) notation.

## 3 MATHEMATICAL MODELLING

In this Section, we describe the design of the model, which offers a holistic approach to the inter-relations between the FSI problem [1, 5, 6, 13, 14, 15, 17] and modelling and simulation of the ultrasonic wave propagation in the ALE variational formulation [5, 6, 7, 8, 9, 10, 11]. This

fully-coupled modelling framework is referred to as the eXtended Fluid-Structure Interaction problem [5, 8, 9, 10, 11, 12, 14].

### 3.1 The eXFSI Problem

*Let us consider, $\hat{v}^D$, and $\hat{u}^D$ are suitable extensions of Dirichlet inflow data. Find the global velocity $\hat{v} \in \{\hat{v}^D + \hat{V}^0_{\hat{\Omega}}\}$, global displacement $\hat{u} \in \{\hat{u}^D + \hat{V}^0_{\hat{\Omega}}\}$, additional velocity $\hat{w} \in \hat{V}^0_{\hat{\Omega}}$, fluid pressure $\hat{p}_f \in \hat{L}^0_{\hat{\Omega}_f}$, global wave displacement $\hat{u}_w \in \hat{V}^0_{\hat{\Omega}}$, and global wave velocity $\hat{v}_w \in \hat{L}_{\hat{\Omega}}$, such that the initial conditions $\hat{v}(0) = \hat{v}^0$, $\hat{u}(0) = \hat{u}^0$, $\hat{u}_w(0) = \hat{u}^0_w$, and $\partial_t \hat{u}_w(0) = \hat{v}^0_w$ are satisfied, and for almost all time $t \in I$ it holds that:*

$$
\begin{aligned}
(\hat{J}\hat{\rho}_f \partial_t \hat{v}, \hat{\phi}^v)_{\hat{\Omega}_f} + (\hat{J}\hat{\rho}_f (\hat{F}^{-1}(\hat{v} - \hat{w}_f)\cdot\hat{\nabla})\hat{v}_f, \hat{\phi}^v)_{\hat{\Omega}_f} + (\hat{J}\sigma_f \hat{F}^{-T}, \hat{\nabla}\hat{\phi}^v)_{\hat{\Omega}_f} & \\
-\langle \hat{g}_f, \hat{\phi}^v\rangle_{\partial\hat{\Omega}_{out}} + (\hat{\rho}_s \partial_t \hat{v}, \hat{\phi}^v)_{\hat{\Omega}_s} + (\hat{J}\hat{\sigma}_s \hat{F}^{-T}, \hat{\nabla}\hat{\phi}^v)_{\hat{\Omega}_s} = 0 \quad \forall \hat{\phi}^v \in \hat{V}^0_{\hat{\Omega}}, & \\
(\hat{J}\hat{\rho}_s \partial_t \hat{v}_w, \hat{\phi}^{v_w})_{\hat{\Omega}_s} - (\hat{J}\hat{\rho}_s (\hat{F}^{-1}\hat{w}_s\cdot\hat{\nabla})\hat{v}_w, \hat{\phi}^{v_w}_s)_{\hat{\Omega}_s} + (\hat{J}\hat{\rho}_s \sigma_{ws}\hat{F}^{-T}, \hat{\nabla}\hat{\phi}^{v_w})_{\hat{\Omega}_s} & \\
-(\hat{J}\hat{f}_s, \hat{\phi}^{v_w})_{\hat{\Omega}_s} + (\hat{J}\hat{\rho}_f \partial_t \hat{v}_w, \hat{\phi}^{v_w})_{\hat{\Omega}_f} - (\hat{J}\hat{\rho}_f (\hat{F}^{-1}\hat{w}_f\cdot\hat{\nabla})\hat{v}_w, \hat{\phi}^{v_w})_{\hat{\Omega}_f} & \\
+(c^2 \hat{J}\hat{\rho}_f (\hat{F}^{-1}\hat{\nabla}\cdot\hat{u}_w)\hat{F}^{-T}, \hat{\nabla}\hat{\phi}^{v_w})_{\hat{\Omega}_f} = 0 \quad \forall \hat{\phi}^{v_w} \in \hat{V}^0_{\hat{\Omega}}, & \\
(\hat{J}\hat{\rho}_s(\partial_t \hat{u}_w - (\hat{F}^{-1}\hat{w}_s\cdot\hat{\nabla})\hat{u}_w - \hat{v}_w), \hat{\phi}^{u_w})_{\hat{\Omega}_s} & \\
+(\hat{J}\hat{\rho}_f(\partial_t \hat{u}_w - (\hat{F}^{-1}\hat{w}_f\cdot\hat{\nabla})\hat{u}_w - \hat{v}_w), \hat{\phi}^{u_w})_{\hat{\Omega}_f} = 0 \quad \forall \hat{\phi}^{u_w} \in \hat{L}_{\hat{\Omega}}, & \\
(\alpha_u \hat{w}, \hat{\phi}^w)_{\hat{\Omega}} - (\alpha_u \hat{\nabla}\hat{u}, \hat{\nabla}\hat{\phi}^w)_{\hat{\Omega}} = 0 \quad \forall \hat{\phi}^w \in \hat{V}^0_{\hat{\Omega}}, & \\
\hat{\rho}_s(\partial_t \hat{u}_s - \hat{v}_s, \hat{\phi}^u)_{\hat{\Omega}_s} + (\alpha_u \hat{\nabla}\hat{w}_f, \hat{\nabla}\hat{\phi}^u)_{\hat{\Omega}_f} = 0 \quad \forall \hat{\phi}^u \in \hat{V}^0_{\hat{\Omega}}, & \\
(\hat{\mathrm{div}}(\hat{J}\hat{F}^{-1}\hat{v}_f), \hat{\phi}^p_f)_{\hat{\Omega}_f} = 0 \quad \forall \hat{\phi}^p_f \in \hat{L}^0_{\hat{\Omega}_f}. &
\end{aligned}
\tag{2}
$$

*Where the transformed Cauchy stress tensor is defined by*

$$\hat{\sigma}_f = -\hat{p}_f \,\mathrm{I} + \hat{\rho}_f \nu_f (\hat{\nabla}\hat{v}_f \hat{F}^{-1} + \hat{F}^{-T}\hat{\nabla}\hat{v}_f^T).$$

*Here, the value of $\hat{w}_f$ is determined from the fluid mesh motion model. Next, the stress tensor is given by*

$$\hat{\sigma}_s = \frac{1}{\hat{J}}\hat{F}\left(2\mu_s \hat{E}_s + \lambda_s \,\mathrm{tr}(\hat{E}_s)\hat{I}\right)\hat{F}^T, \quad \hat{E}_s = \frac{1}{2}\left(\hat{\nabla}\hat{u}_s\hat{F}^{-1} + \hat{F}^{-T}\hat{\nabla}\hat{u}_s^T\right).$$

*where, $\lambda_s$ and $\mu_s$ are Lamé parameters. Finally, for the wave propagation problem, the linearized stress tensor is given by*

$$\hat{\sigma}_{ws} = \frac{1}{\hat{J}}\hat{F}\left(2\mu_s \hat{E}_{ws} + \lambda_s \,\mathrm{tr}(\hat{E}_{ws})\hat{I}\right)\hat{F}^T, \quad \hat{E}_{ws} = \frac{1}{2}\left(\hat{\nabla}\hat{u}_{ws}\hat{F}^{-1} + \hat{F}^{-T}\hat{\nabla}\hat{u}_{ws}^T\right).$$

*Here, $\mu_s$ and $\lambda_s$ are the Lamé coefficients for the solid. The value of $\hat{w}_s$ is determined from the FSI problem.*

In the next step, the variational formulation is prescribed in an arbitrary fixed reference domain. Noteworthy, all the coupling conditions are satisfied in an accurate variational fashion on the continuous level. Solving the eXFSI problem in a monolithic way, we avoid the difficulties with the so-called added-mass effect. For the time discretization we employ the Rothe (horizontal line) strategy. Here, the temporal discretization is performed by using the finite difference scheme. Specifically, we use the one step-$\theta$ schemes, focusing on the shifted Crank-Nicolson schemes. For the spatial discretization, we refer to a standard Galerkin finite element approach. We use the finite element pair $Q_2^c/P_1^{dc}$ for the fluid flow. For the structural deformations and the coupled wave propagation problems, we use the element $Q_2^c$. The nonlinear problem is solved using a Newton-like method. The Jacobian is derived by the exact linearization. Thereby, we ensure robustness, while opting for rapid convergence. The implementation is accomplished via the software library package DOPELIB [21] (based on `deal.ii` [22]). Note, we refer to the direct solver UMFPACK [23] for solution of the linear equation systems at each Newton step.

## 4 NUMERICAL TEST

The numerical tests presented here aim at mimicing the physical behaviour of the FSI-wave propagaton system. Specifically, we aim at mimicing the damage identification system. For this, we closely analyze the wave patterns as wave propagates through a solid domain in motion. We consider the deformable elastic structure, part of which is immersed in fluid. Both parts of the structure feature fluid detached inclusions. Importanly, for comparability, these two inclusions are located symmetrically with respect to the source of the signal. This allows us to contrast the wave propagation patterns in a structure in motion and the one that is steady (cf. Figure 1). For a reference, we also illustrate the case with static fluid case. The test cases share the same geometric configuration and all feature the non-vanishing disc-shaped input signal. Space-discretisation is done via one global refinement iteration. Accordingly, we refine the geometrical structure into $66,450$ quadratic-mesh cells. Here each cell have $165$ local degrees of freedom (DoFs) for the eXFSI problem. The time discretisation is done by the well-known shifted Crank-Nicolson scheme. To enhance quality of the numerical solution at a particular time segment, we apply uniform time discretisation within a segment, which is different among the segments. Specifically, we distinguish 3 time segments: $I_1 = [0; 2)$, $I_2 = [2; 2.01125)$, and $I_3 = [2.01125; 2.51125]$. Each segment $I_n$, $n = 1, 2, 3$, is discretised via segment-specific time step $k_n$. Here, $k_1 = 0.2$ s, $k_2 = 0.000125$ s, and $k_3 = 0.05$ s. The global tolerance is set to $1 \times 10^{-8}$; the relative tolerance for the Newton iteration is set to $1 \times 10^{-10}$.

### 4.1 Baseline configuration

The domain is illustrated in Figure 1, where the notations and subdomains are depicted. At the geometric center $(0; 0)$ of the solid plate, there is a non-vanishing disc-shaped piezoelectric actuator $\hat{f}_s(\hat{x}, t)$ with a radius $\hat{r}_{f_s}$ of $7.5$ mm [5, 6, 8]. It is used for the purpose of the excitation of a burst Lamb wave package. In particular, in our simulations, we refer to a five-cycle Lamb wave package, which has two main displacement field components $\hat{u}_{w_x}$ and $\hat{u}_{w_y}$ in the plane. Besides, we choose the upper right corner of the structure with $(0.25, 0.5)$ as a control point to measure the deflections initiated by the FSI effect. We introduce three eXFSI test cases that are

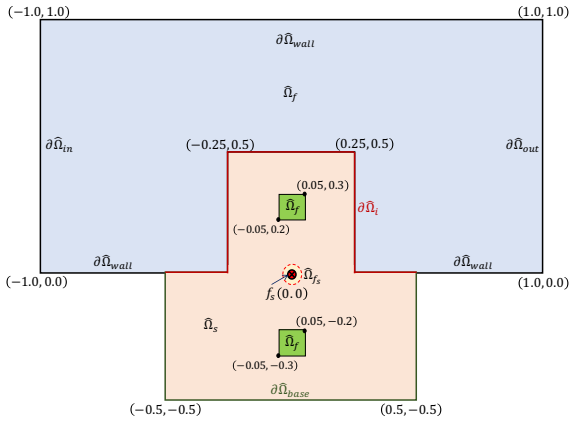


Figure 1: The reference (initial) configuration for 2D eXFSI test model with a disc-shaped force $f_s$ at $(0, 0)$.

treated with different inflow velocities (see Table-1).

Table 1: Parameter setting for the eXFSI test cases.

| Parameter | eXFSI-0 | eXFSI-1 | eXFSI-2 |
|---|---|---|---|
| Structure model | STVK | STVK | STVK |
| $\rho_f$ $[10^3\ kgm^{-3}]$ | 1 | 1 | 1 |
| $\rho_s$ $[10^3\ kgm^{-3}]$ | 1 | 1 | 10 |
| $\nu_f[10^{-3}\ m^2s^{-1}]$ | 1 | 1 | 1 |
| $c\ [10^3\ ms^{-1}]$ | 1 | 1 | 1 |
| $\nu_s$ | 0.4 | 0.4 | 0.4 |
| $\mu_s$ $[10^6\ kgm^{-1}\mathrm{s}^{-2}]$ | 0.50 | 0.50 | 0.50 |
| $U_m[ms^{-1}]$ | 0 | 0.2 | 1.0 |

### 4.2 Initial and boundary conditions

The boundary conditions are given by:

1. A constant parabolic inflow profile is prescribed at the left inlet as

$$v(0, y) = 1.5U_m \frac{4y(H - y)}{H^2}, \tag{3}$$

where $U_m$ is the mean inflow velocity and the maximum inflow velocity in $1.5U_m$.

2. At outlet, zero-stress $\sigma.n = 0$ is realized by using the 'do-nothing' approach in the variational formulation. Along the upper and lower boundary, the usual 'no-slip' condition is used for the velocity. Bottom end of "⊥" shaped solid is considered rigid.

We consider the following initial conditions for the FSI problem:

$$v_f(t;0,y) = \begin{cases} v_f(0,y)\frac{1-cos(\frac{\pi}{2}t)}{2}, & t < 2.0, \\ \\ v_f(0,y), & t \geq 2.0, \end{cases} \tag{4}$$

and the following initial conditions for the WpFSI problem:

$$\begin{aligned} \hat{u}_{w_s}(\hat{x},0) = 0, \quad \hat{u}_{w_f}(\hat{x},0) = 0, \\ \partial_t \hat{u}_{w_s}(\hat{x},0) = 0, \quad \partial_t \hat{u}_{w_f}(\hat{x},0) = 0. \end{aligned} \tag{5}$$

### 4.3 Simulation results

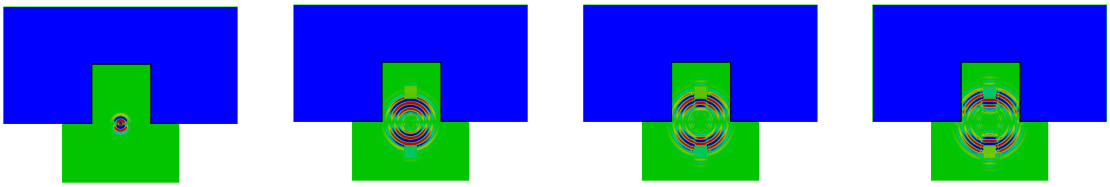

(i) $t = 2.5$ ms (ii) $t = 6$ ms (iii) $t = 6.88$ ms (iv) $t = 7.25$ ms

(a) Test case eXFSI-0.

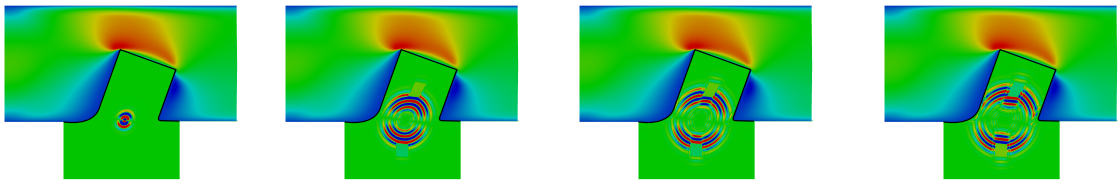

(i) $t = I_1 + 2.5$ ms (ii) $t = I_1 + 6$ ms (iii) $t = I_1 + 6.88$ ms (iv) $t = I_1 + 7.25$ ms

(b) Test case eXFSI-1.

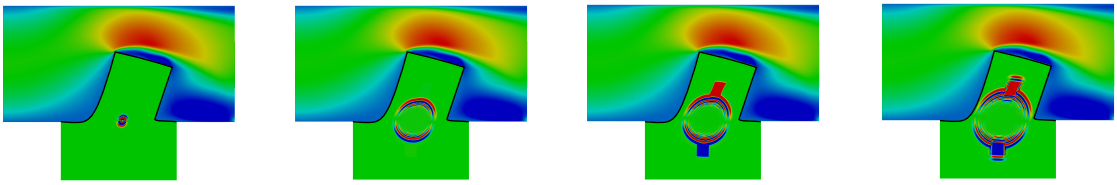

(i) $t = I_1 + 3.5$ ms (ii) $t = I_1 + 12.5$ ms (iii) $t = I_1 + 14$ ms (iv) $t = I_1 + 16.5$ ms

(c) Test case eXFSI-2.

Figure 2: The displacement field component $\hat{u}_{x_2}$ with fluid velocity field at different time.

This test configuration comprises the baseline configuration extended by adding the two liquid inclusions (subdomains). As illustrated in Figure 1, the two subdomains are located symmetrically with respect to the actuator. Importantly, one subdomain is located in the part of the solid that is exposed to the fluid flow. The other subdomain – in the part of the solid, which is not exposed. This setup allows us to contrast the effects of the same signal in a structure in motion and in a fixed structure. The results for eXFSI-1 case are illustrated in Figure 2.

Figure 2 illustrates the numerical simulation results for the test case eXFSI-0, eXFSI-1 and eXFSI-2. For each test case we present 4 time-snapshots, which allows for tracking the patterns alterations. The reference case, eXFSI-0, depicts the case with no fluid flow i.e. $U_m = 0.0$ $ms^{-1}$ and thus structural deformations. This case mimics the performance of the off-live SHM system. We observe symmetrical propagation of the wave, where the presence of the fluid inclusion is clearly identified. Nest, we move to the on-live SHM system (test case eXFSI-1). Here, the fluid flow of velocity $U_m = 0.02$ $ms^{-1}$ deforms the solid structure, which, in turn, squeezes the wave pattern. Both eXFSI-0 and eXFSI-1 feature the same material properties.

Next, we presents the results for alternative material and higher fluid velocity $U_m = 1.0$ $ms^{-1}$ (test case eXFSI-2). Again, we observe a solid deformation under the flow. As wave reaches the liquid inclusion, it creates reflections. At the fluid-solid interface, the further reflections occur. These are prominent compared to the case eXFSI-1. The differences come into play due to alternative solid-to-fluid density ratio. The higher the ratio, the higher the wave amplitude in the liquid subdomain. This numerical results are in line with the experimental data. For example, in [19, 20] the ultrasonic wave propagation is tracked in a blade by means of image processing. As a final note, the present research results should be considered as a numerical benchmark for the SHM system.

## 5 CONCLUDING REMARKS

In the present paper, we introduce the new state-of-the-art mathematical model that describes the wave propagation through media in motion. Numerical solution demonstrates the ability of the model to successfully identify the inclusion in the solid by tracking the wave patterns as wave propagates. In this case, we use the inclusion to mimic the damage for the purpose of demonstration. The real-life applications would require larger set of potential damage-inducing materials to be tested. The set of materials differs across applications. In our model, this would be translated in the alterations of the material properties calibration. Another important future extensions include definition of changes associated with alternative structural (and environmental) characteristics and development of the noise detection function (NDF) that translates the structural conditions into the output sensor data.

## REFERENCES

[1] H. J. Bungartz, M. Miriam and M. Schaefer (Eds.). *Fluid-Structure Interaction-II: Modelling, Simulation, Optimization*. Lecture Notes in Computational Science and Engineering, Vol. 73. Springer, 2010.

[2] G. P. Galdi and R. Rannacher, (Eds.). *Fundamental Trends in Fluid-Structure Interaction*. Series on Contemporary Challenges in Mathematical Fluid Dynamics and Its Applications, Vol. 1. World Scientific Publishing Co. Pte. Ltd., 2010.

[3] Y. Bazilevs, K. Takizawa and T. E. Tezduyar. *Computational Fluid-Structure Interaction: Methods and Applications*. Wiley Series in Computational Mechanics, John Wiley & Sons Ltd., 2013.

[4] T. Richter. *Fluid Structure Interactions: Mathematical Analysis and Finite Elements*. Lecture Notes in Computational Science and Engineering, Springer, 2017.

[5] B.S.M. Ebna Hai. *Finite Element Approximation of Ultrasonic Wave Propagation under Fluid-Structure Interaction for Structural Health Monitoring Systems.* Doctoral Thesis, Department of Mechanical Engineering, Helmut Schmidt University - University of the Federal Armed Forces Hamburg, Germany, Oct 27, 2017.

[6] B.S.M. Ebna Hai and M. Bause. *Adaptive Multigrid Methods for Fluid-Structure Interaction (FSI) Optimization in an Aircraft and design of integrated Structural Health Monitoring (SHM) Systems.* In proceedings of: the $2^{nd}$ ECCOMAS Young Investigators Conference (YIC2013), Bordeaux, France, Sept 02–06, 2013.

[7] B.S.M. Ebna Hai and M. Bause. *Finite Element Model-based Structural Health Monitoring (SHM) Systems for Composite Material under Fluid-Structure Interaction (FSI) Effect*. In proceedings of: the $7^{th}$ European Workshop on Structural Health Monitoring (EWSHM2014), July 08–11, 2014, Nantes, France. In: The e-Journal of Nondestructive Testing & Ultrasonics, NDT.net issue (ISSN: 1435–4934), Vol. 20, Issue 2 (Feb 2015), pp 1380–1387, 2015.

[8] B.S.M. Ebna Hai and M. Bause. *Adaptive Multigrid Methods for An Integrated Structural Health Monitoring (SHM) Systems for Composite Material with Fluid-Structure Interaction (FSI) Effect.* The SIAM Conference on Computational Science and Engineering (CSE15), Salt Lake City, Utah, USA, March 14–18, 2015.

[9] B.S.M. Ebna Hai and M. Bause. *Adaptive Multigrid Methods for eXtended Fluid-Structure Interaction (eXFSI) Problem: Part I - Mathematical Modelling*. In proceedings of: the ASME International Mechanical Engineering Congress & Exposition (IMECE2015), Vol. 7B, No. IMECE2015–53265, pp V07BT09A039/1–10, Houston, Texas, USA, Nov 13–19, 2015.

[10] B.S.M. Ebna Hai and M. Bause. *Finite Element Model-based Structural Health Monitoring (SHM) Systems with Fluid-Structure Interaction (FSI) Effect*. In proceedings of: the $11^{th}$ International Workshop on Structural Health Monitoring, Sept 12–14, Stanford University, CA, USA. In: F-K. Chang and F. Kopsaftopoulos (Ed.), *"Structural Health Monitoring 2017: Real-Time Material State Awareness and Data-Driven Safety Assurance"*, DEStech Publications Inc., USA, Vol. 1, pp 580–587, 2017.

[11] B.S.M. Ebna Hai, M. Bause and P. Kuberry. *Finite Element Approximation of the eXtended Fluid-Structure Interaction (eXFSI) Problem*. In proceedings of: the ASME Fluids Engineering Division Summer Meeting, Vol. 1A, No. FEDSM2016–7506, pp V01AT11A001/1–12, Washington, D.C., USA, July 10–14, 2016.

[12] B.S.M. Ebna Hai and M. Bause. *Finite Element Approximation of Fluid-Structure Interaction (FSI) Problem with Coupled Wave Propagation*. In proceedings of: the $88^{th}$ GAMM Annual Meeting of the International Association of Applied Mathematics and Mechanics, March 6–10, 2017, Weimar, Germany. In: *"PAMM - Proceedings in Applied Mathematics and Mechanics"*, WILEY-VCH Verlag GmbH & Co. KGaA, Weinheim, Vol. 17, Issue 1, pp 511-512, 2018.

[13] B.S.M. Ebna Hai. *Numerical Approximation of Fluid Structure Interaction (FSI) Problem*. In proceedings of: the ASME Fluids Engineering Division Summer Meeting (FEDSM2013), Vol. 1A, No. FEDSM2013–16013, pp V01AT02A001/1–10, Incline Village, Nevada, USA, July 7–11, 2013.

[14] B.S.M. Ebna Hai and M. Bause. *Finite Element Approximation of Fluid Structure Interaction (FSI) Optimization in Arbitrary Lagrangian-Eulerian Coordinates*. In proceedings of: the ASME International Mechanical Engineering Congress & Exposition (IMECE2013), Vol. 7B, No. IMECE2013–62291, pp V07BT08A034/1–8, Nov 13–21, San Diego, California, USA, November 15–21, 2013.

[15] B.S.M. Ebna Hai and M. Bause. *Adaptive Finite Elements Simulation Methods and Applications for Monolithic Fluid-Structure Interaction (FSI) Problem*. In proceedings of: the ASME $4^{th}$ Joint US-European Fluids Engineering Division Summer Meeting, Vol. 1B, No. FEDSM2014–21379, pp V01BT12A003/1–10, Chicago, Illinois, USA, August 3–7, 2014.

[16] B.S.M. Ebna Hai and M. Bause. *Finite Element Approximation of Wave Propagation in Composite Material With Asymptotic Homogenization*. In proceedings of: the ASME Turbo Expo: Turbine Technical Conference and Exposition, Vol. 7A, No. GT2014–26314, pp V07AT28A009/1-10, Düsseldorf, Germany, June 16–20, 2014.

[17] T. Wick. "Adaptive Finite Element Simulation of Fluid-Structure Interaction with Application to Heart-Valve Dynamics", *Doctoral dissertation,* University of Heidelberg, Germany, 2011.

[18] S. Frei, T. Richter, and T. Wick. "Long-term simulation of large deformation, mechano-chemical fluid-structure interactions in ALE and fully Eulerian coordinates", *Journal of Computational Physics,* Vol. 321, pp 874–891, 2016.

[19] B. Park, H. Sohn, C-M. Yeum and T. C. Truong. "Laser ultrasonic imaging and damage detection for a rotating structure", *Structural Health Monitoring,* Vol. 12, Issues 5–6, pp 494–506, 2013.

[20] B. Park, and H. Sohn. "Instantaneous damage identification and localization through sparse laser ultrasonic scanning", *In proceedings of: the 7$^{th}$ European Workshop on Structural Health Monitoring (EWSHM2014),* Nantes, France, July 08–11, 2014.

[21] C. Goll, T. Wick and W. Wollner. DOPELIB*: Differential Equations and Optimization Environment; A Goal Oriented Software Library for Solving PDEs and Optimization Problems with PDEs*. Archive of Numerical Software, Vol. 5, Issue 2, pp 1-14, 2012.

[22] W. Bangerth, R. Hartmann and G. Kanschat. `deal.II`*: a general-purpose object-oriented finite element library*. ACM Transactions on Mathematical Software, Vol. 33, Issue 4, pp 24/1–27, 2007.

[23] T. A. Davis and I. S. Duff. *An unsymmetric-pattern multifrontal method for sparse LU factorization.* SIAM Journal on Matrix Analysis and Applications, Vol. 18, Issue 1, pp 140–158, 1997.